Inflammatory macrophage migration requires MMP-9 activation by plasminogen in mice

Yanqing Gong, Erika Hart, Aleksey Shchurin, and Jane Hoover-Plow

Joseph J. Jacobs Center for Thrombosis and Vascular Biology, Department of Cardiovascular Medicine, and Department of Molecular Cardiology, Cleveland Clinic Lerner Research Institute, Cleveland, Ohio, USA.

Inflammation plays a critical role in the development of cardiovascular diseases. Infiltration of leukocytes to sites of injury requires their exit from the blood and migration across basement membrane; this process has been postulated to require remodeling of the ECM. Plasminogen (Plg) is a protease that binds to the ECM and, upon conversion to plasmin, degrades multiple ECM proteins. In addition, plasmin directly activates MMPs. Here, we used *Plg*$^{-/-}$ mice to investigate the role of Plg in inflammatory leukocyte migration. After induction of peritonitis by thioglycollate injection, we found that *Plg*$^{-/-}$ mice displayed diminished macrophage trans-ECM migration and decreased MMP-9 activation. Furthermore, injection of the active form of MMP-9 in *Plg*$^{-/-}$ mice rescued macrophage migration in this model. We used periaortic application of $CaCl_2$ to induce abdominal aortic aneurysm (AAA) and found that *Plg*$^{-/-}$ mice displayed reduced macrophage infiltration and were protected from aneurysm formation. Administration of active MMP-9 to *Plg*$^{-/-}$ mice promoted macrophage infiltration and the development of AAA. These data suggest that Plg regulates macrophage migration in inflammation via activation of MMP-9, which, in turn, regulates the ability of the cells to migrate across ECM. Thus, targeting the Plg/MMP-9 pathway may be an attractive approach to regulate inflammatory responses and AAA development.

Introduction

Cardiovascular disease (CVD) is the leading cause of mortality in the United States and is responsible for nearly 50% of adult deaths. Numerous studies (reviewed in ref. 1) document the association of inflammatory markers with CVD, suggesting that inflammation is a critical factor in the initiation and progression of CVD. Central to the inflammatory response is leukocyte recruitment to the sites of injury. Leukocyte recruitment following inflammation is characterized by neutrophil and monocyte migration to the site of injury, where neutrophils are often the first cells to arrive, followed by macrophages. Leukocyte recruitment requires exit of cells from the blood and their migration across basement membranes and into the injured tissue (2). It has long been postulated that these migratory events are dependent upon proteolytic remodeling of the ECM (3, 4).

Abdominal aortic aneurysm (AAA) is a chronic degenerative condition that is characterized by chronic inflammation, segmental weakening and dilation of the vessel wall, and destructive remodeling of ECM (5). Studies of human AAA tissue have identified extensive infiltration of inflammatory cells in both the media and adventitia, and macrophages and lymphocytes are the predominant leukocytes that initiate aneurysm formation by producing proinflammatory cytokines and proteolytic enzymes (6). Proteases, including plasminogen (Plg), and MMPs, especially MMP-2, MMP-9, and MMP-12, have been implicated in the degradation of ECM that leads to AAA development (7, 8).

Plg, the zymogen for plasmin, plays a major role in inflammatory cell recruitment. Plg, produced by the liver and by certain other tissues (9, 10), circulates at high concentrations (2 μM) in plasma. Plg is converted to active plasmin by tissue Plg activator (tPA) or urokinase Plg activator (uPA). The major inhibitors of the Plg system are Plg activator inhibitor–1 (PAI-1) and α_2-antiplasmin. Using gene-targeted mice, studies have shown that the Plg system regulates leukocyte recruitment in inflammation (11–14) as well as in inflammation-associated CVD, including AAA (15–17). Mice deficient in uPA (18, 19) or overexpressing PAI-1 (20) are protected from aneurysm formation, suggesting that Plg system and its regulated macrophage infiltration are essential to aneurysm development. Plg is able to directly bind to the ECM and upon its conversion to plasmin can degrade multiple ECM proteins (21). Plasmin can also activate other ECM-degrading proteinases, such as MMP-3, MMP-9, MMP-12, and MMP-13 (22), that may contribute to Plg-regulated leukocyte migration. However, in vivo evidence for this mechanism of Plg-dependent ECM turnover is still lacking.

To elucidate the mechanism underlying Plg-regulated leukocyte migration in vivo, we designed experiments using 2 mouse models: first a simple thioglycollate-induced peritoneal inflammatory model and then a more complex inflammatory atherosclerotic $CaCl_2$-induced AAA model. The results presented here show that MMP-9 activation is required for Plg-dependent macrophage trans-ECM migration and progression of AAA.

Results

Plg activation is required for recruitment of macrophages but not neutrophils. The effect of Plg deficiency on leukocyte migration was evaluated in a peritonitis model induced by an i.p. injection of thioglycollate, an extensively used inflammatory stimulus that induces the recruitment of neutrophils and macrophages to the peritoneal cavity. In this model, neutrophil number reaches a maximum at 6–8 hours, while macrophages emigrate with a slow time course, reaching a maximum at 72 hours and remaining at this level for at least 96 hours (12, 23). Consistent with previous studies (12), Plg defi-

Nonstandard abbreviations used: AAA, abdominal aortic aneurysm; act-MMP-9, active form of MMP-9; CVD, cardiovascular disease; MCP-1, monocyte chemoattractant protein–1; PAI-1, Plg activator inhibitor–1; PLF, peritoneal lavage fluid; Plg, plasminogen; proMMP-9, proenzyme form of MMP-9; tPA, tissue Plg activator; uPA, urokinase Plg activator.

Conflict of interest: The authors have declared that no conflict of interest exists.

Citation for this article: *J. Clin. Invest.* **118**:3012–3024 (2008). doi:10.1172/JCI32750.

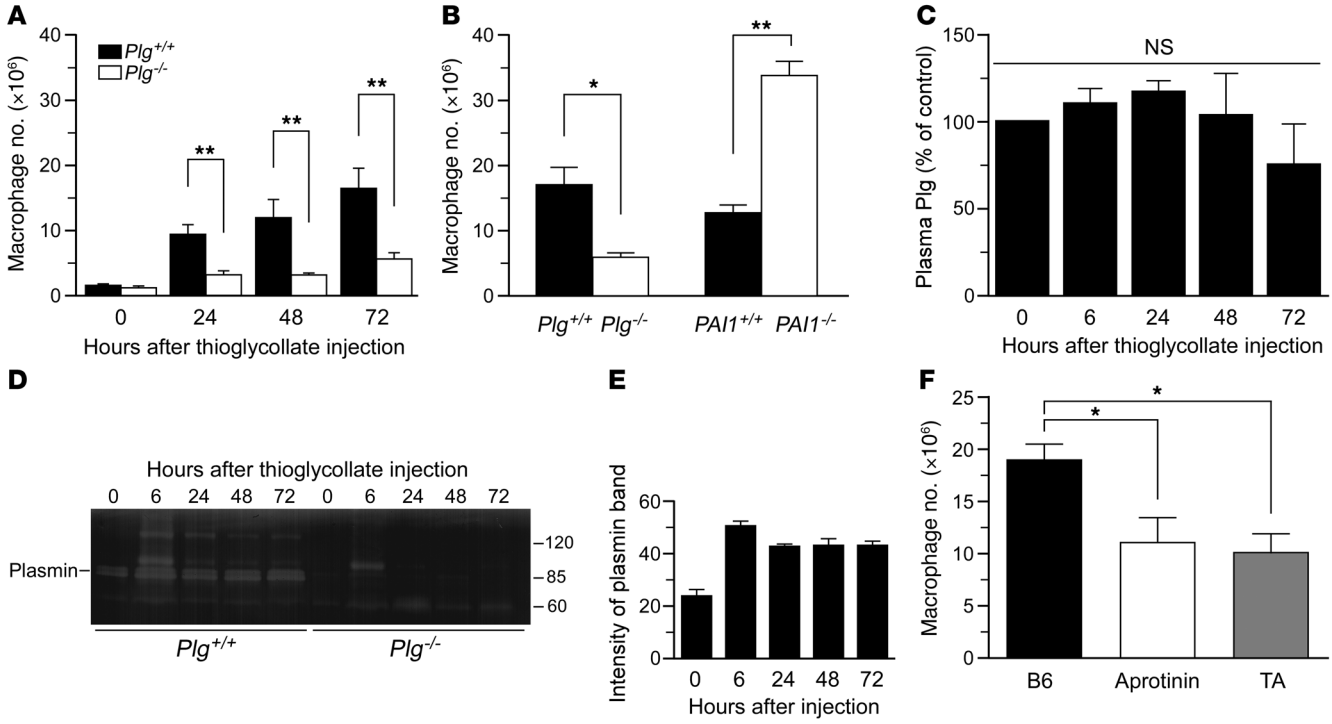

Figure 1

Plg activation is required for macrophage recruitment. (**A**) Macrophage recruitment in $Plg^{+/+}$ and $Plg^{-/-}$ mice after thioglycollate injection (n = 3–7). (**B**) Recruitment of macrophages is suppressed in $Plg^{-/-}$ mice and enhanced in $PAI1^{-/-}$ mice (n = 9–22 mice per group). (**C**) Plg in plasma of $Plg^{+/+}$ mice (n = 3) is unaffected by thioglycollate treatment. (**D**) Plasmin (83 kDa) activity in PLF was measured by casein zymography. (**E**) Intensity of plasmin bands in $Plg^{+/+}$ PLF (3 independent assays). (**F**) Aprotinin and tranexamic acid (TA) reduce thioglycollate-induced macrophage recruitment in $Plg^{+/+}$ mice (n = 8–10). *P < 0.05, **P < 0.01.

ciency suppressed macrophage recruitment to the peritoneal cavity in a time-dependent manner (Figure 1A). At 72 hours, macrophage recruitment was reduced by 65% compared with that in age- and sex-matched $Plg^{+/+}$ littermates. In agreement with these findings, macrophage recruitment was significantly increased in mice with deficiency of PAI-1, the primary endogenous Plg activator inhibitor (Figure 1B). These data indicate a central role of Plg in macrophage recruitment in peritoneal inflammation. Consistent with previous findings (12), neutrophil recruitment (cells × 10^6, mean ± SEM) was not altered in $Plg^{-/-}$ mice (2.5 ± 0.7; n = 9) compared with $Plg^{+/+}$ mice (2.5 ± 0.6; n = 9), implying that different mechanisms are involved in neutrophil and macrophage migration.

To further investigate whether the activation of Plg to plasmin is involved in macrophage recruitment in the thioglycollate model, we examined both Plg protein level and the activity of plasmin after thioglycollate injection. There were no significant changes in plasma Plg levels after thioglycollate injection in $Plg^{+/+}$ mice (Figure 1C). In the peritoneal lavage fluid (PLF), plasmin activity, detected on casein gels, increased 2-fold 6 hours after thioglycollate stimulation, and the increase was maintained for 72 hours (Figure 1, D and E). Of interest, a second unidentified protease band with a molecular weight higher than that of plasmin (~95 kDa) was detected at the 6-hour time point in both wild-type and Plg-deficient mice. These results suggest that Plg activation to plasmin may be involved in macrophage recruitment in the thioglycollate model. This interpretation was corroborated by the suppression of macrophage recruitment after $Plg^{+/+}$ mice were treated with tranexamic acid, an inhibitor of Plg binding to cell surfaces, and aprotinin, a potent inhibitor of plasmin activity (Figure 1F). Together, these data indicate that Plg and its activation to plasmin are important mediators of inflammation-induced macrophage recruitment.

Macrophages accumulate in peritoneal tissue in $Plg^{-/-}$ mice after thioglycollate injection. There are several possible mechanisms by which Plg deficiency could suppress macrophage recruitment. First, Plg deficiency may inhibit the production of monocytes, the source of macrophages. However, a previously published study (12) showed that blood monocyte levels from 0 to 96 hours after thioglycollate stimulation in $Plg^{-/-}$ and $Plg^{+/+}$ mice are similar. Second, Plg deficiency may alter the resident macrophages in the peritoneal cavity or the origin of the macrophages after stimulation with thioglycollate. To determine whether the origin of the macrophages is different in $Plg^{+/+}$ and $Plg^{-/-}$ mice, mice were injected intravenously with PKH2-PCL 24 hours prior to thioglycollate administration to label phagocytes. Peritoneal cells were collected at 72 hours, and the percentage of PKH2-PCL–labeled macrophages was determined as described in Methods. The results (80% ± 10% in $Plg^{+/+}$ mice, 82% ± 5% in $Plg^{-/-}$ mice) indicate that most peritoneal macrophages are recruited from blood, consistent with findings of other studies (23, 24), and that there was no difference between $Plg^{+/+}$ and $Plg^{-/-}$ mice. Hence, the origin of the peritoneal macrophages is similar in the 2 genotypes in this model.

As a third potential mechanism for decreased macrophage recruitment, Plg deficiency may block macrophage migration across the peritoneal tissue in response to the inflammatory stimulus. To test

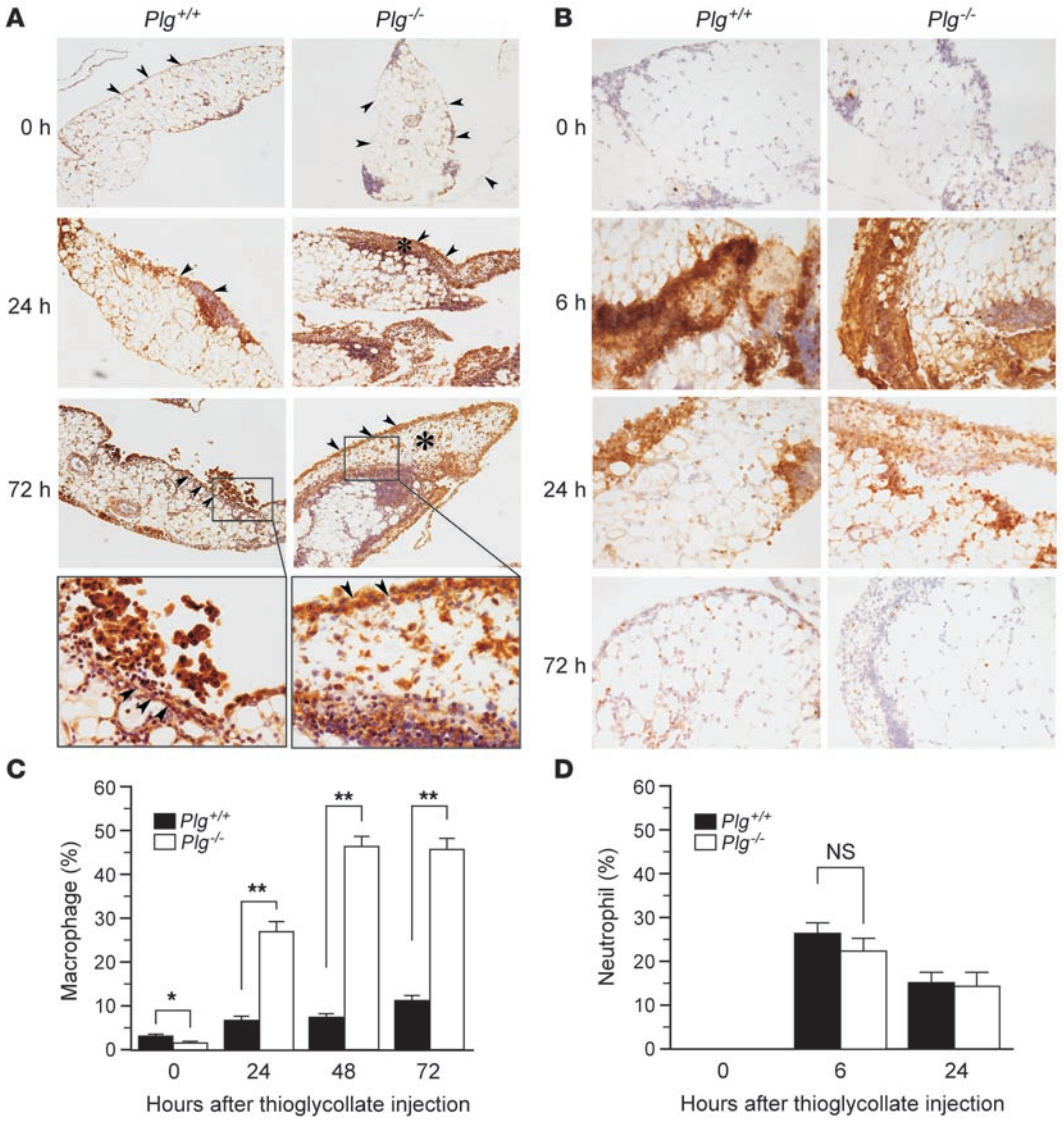

Figure 2
Trans-ECM migration of macrophages, but not neutrophils, is blocked in peritoneal tissue of *Plg*$^{-/-}$ mice. Peritoneal tissue was dissected and examined after thioglycollate treatment. (**A**) Macrophage (Mac-3 antibody). Original magnification, ×100; insets, ×400. Arrowheads indicate mesothelial layer; asterisk indicates macrophage accumulation area. (**B**) Neutrophil (neutrophil antibody). Original magnification, ×200. (**C** and **D**) Macrophage and neutrophil distribution (expressed as percentage of tissue area) in peritoneal tissue (n = 5–6). *P < 0.05, **P < 0.01.

this possibility, peritoneal tissue (25) was harvested from *Plg*$^{+/+}$ and *Plg*$^{-/-}$ mice and examined. Sections were immunohistochemically stained to distinguish macrophages and neutrophils. Macrophage migration in response to thioglycollate stimulation was blocked in the peritoneal tissue in *Plg*$^{-/-}$ mice (Figure 2A). The number of macrophages that accumulated was 4-fold higher in the peritoneal tissue in *Plg*$^{-/-}$ compared with *Plg*$^{+/+}$ mice (Figure 2C). Moreover, the macrophages in the *Plg*$^{-/-}$ mice accumulated in the submesothelial layer of the peritoneal tissue as early as 24 hours after thioglycollate stimulation. At 48–72 hours, the submesothelial layer became engorged, with edema and the accumulation of a large number of macrophages (Figure 2A). The mesothelial layer was discontinuous in tissue from the *Plg*$^{+/+}$ mice, and macrophages were present on the cavity side of the layer. In the *Plg*$^{-/-}$ mice, the mesothelial layer was intact, and macrophages accumulated on the tissue side (Figure 2A, insets). These data indicate that the impaired movement of macrophages in *Plg*$^{-/-}$ mice is due to a diminished ability of macrophages to transmigrate through the ECM (especially in mesothelium) and exit the tissue into the peritoneal cavity. In contrast to the distribution pattern for macrophages, the number of neutrophils in the peritoneal tissue peaked at 6 hours, was reduced by 24 hours, and disappeared by 72 hours, and there was no difference in the number of neutrophils in the *Plg*$^{+/+}$ and *Plg*$^{-/-}$ mice during the 6–24 hours after thioglycollate stimulation (Figure 2, B and D). In summary, these data indicate that Plg deficiency inhibits macrophage migration, but not neutrophil migration, across the ECM in the peritoneal tissue.

Collagen content in the peritoneal tissue is altered in Plg$^{-/-}$ *mice after thioglycollate stimulation*. To test whether the ECM is involved in the impaired macrophage migration across the peritoneal tissue of *Plg*$^{-/-}$ mice, we first investigated the distribution and expression

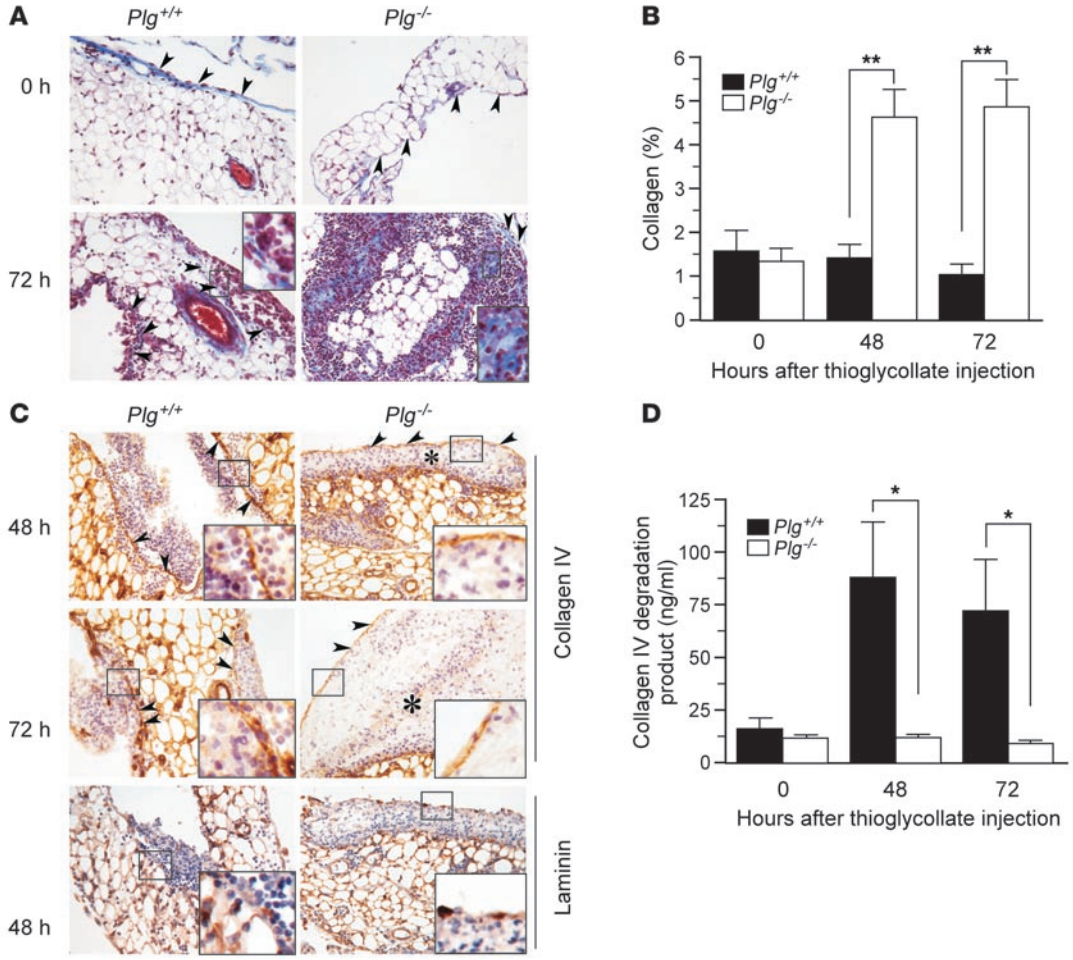

Figure 3
Collagen content is altered in thioglycollate-injected $Plg^{-/-}$ mice. (**A**–**C**) Peritoneal tissue from $Plg^{+/+}$ and $Plg^{-/-}$ mice was stained after thioglycollate treatment. (**A**) Collagen stained blue by Masson's trichrome. Original magnification, ×200; insets, ×400. Arrowheads indicate mesothelial layer. (**B**) Total collagen as percentage of total section area (n = 4–6). $^{**}P < 0.01$. (**C**) Collagen IV and laminin. Arrowheads indicate mesothelial layer; asterisk indicates macrophage accumulation area (n = 4–6). Original magnification, ×200; insets, ×400. (**D**) Collagen IV degradation. PLF of mice was isolated after thioglycollate injection, and soluble collagen IV degradation products were quantified by ELISA (n = 4). $^{*}P < 0.05$.

of collagen, a major component of ECM. As detected by Masson's trichrome staining, there was no initial difference in total collagen (bright blue) present in the $Plg^{-/-}$ and $Plg^{+/+}$ mice (0 hours). The collagen was located mainly in mesothelial layer and around the arterioles in the peritoneal tissue. Thioglycollate stimulation did not alter collagen distribution and content in $Plg^{+/+}$ mice. However, abundant collagen (3-fold increase; Figure 3, A and B) was deposited in the area of macrophage accumulation in $Plg^{-/-}$ mice at 72 hours after thioglycollate injection. The pattern of enhanced collagen deposition was also observed at 48 hours but was not detected in the early stages of the inflammatory response (6 or 24 hours after thioglycollate injection; data not shown) in the $Plg^{-/-}$ mice. These data indicate that Plg deficiency increases collagen deposition with a spatiotemporal correspondence to macrophage accumulation, suggesting that collagen may serve as a barrier to macrophage migration. Excess collagen accumulation in $Plg^{-/-}$ mice may impair macrophage migration through the peritoneal tissue into the peritoneal cavity.

The basement membrane underlying mesothelial cells is a continuous layer composed mainly of collagen IV and laminin (26). We visualized the collagen IV and laminin in the peritoneal tissue by immunostaining (Figure 3C). In untreated $Plg^{+/+}$ and $Plg^{-/-}$ mice, collagen IV formed a continuous layer in the mesothelium surrounding the peritoneal tissue. In the $Plg^{+/+}$ mice stimulated with thioglycollate, a large number of macrophages successfully migrated across the collagen IV layer, and at 72 hours the collagen barrier was discontinuous in the area of macrophage accumulation. In the $Plg^{-/-}$ mice, the macrophages failed to migrate across the collagen IV layer of the mesothelium. The collagen IV layer remained intact (see inset), and macrophages accumulated in the submesothelial layer. To quantify the collagen IV disruption in $Plg^{+/+}$ and $Plg^{-/-}$ mice during peritoneal inflammation, collagen IV–soluble degradation products in PLF were measured by an ELISA (Figure 3D). A 2- to 3-fold increase in the soluble collagen IV concentration was detected in $Plg^{+/+}$ mice 48 and 72 hours after thioglycollate injection, compared with no increase in $Plg^{-/-}$ mice, confirming that Plg is required for collagen IV degradation in the thioglycollate inflammatory model. Furthermore, laminin distribution (dark brown) was discontinuous along the mesothelial layer (see inset),

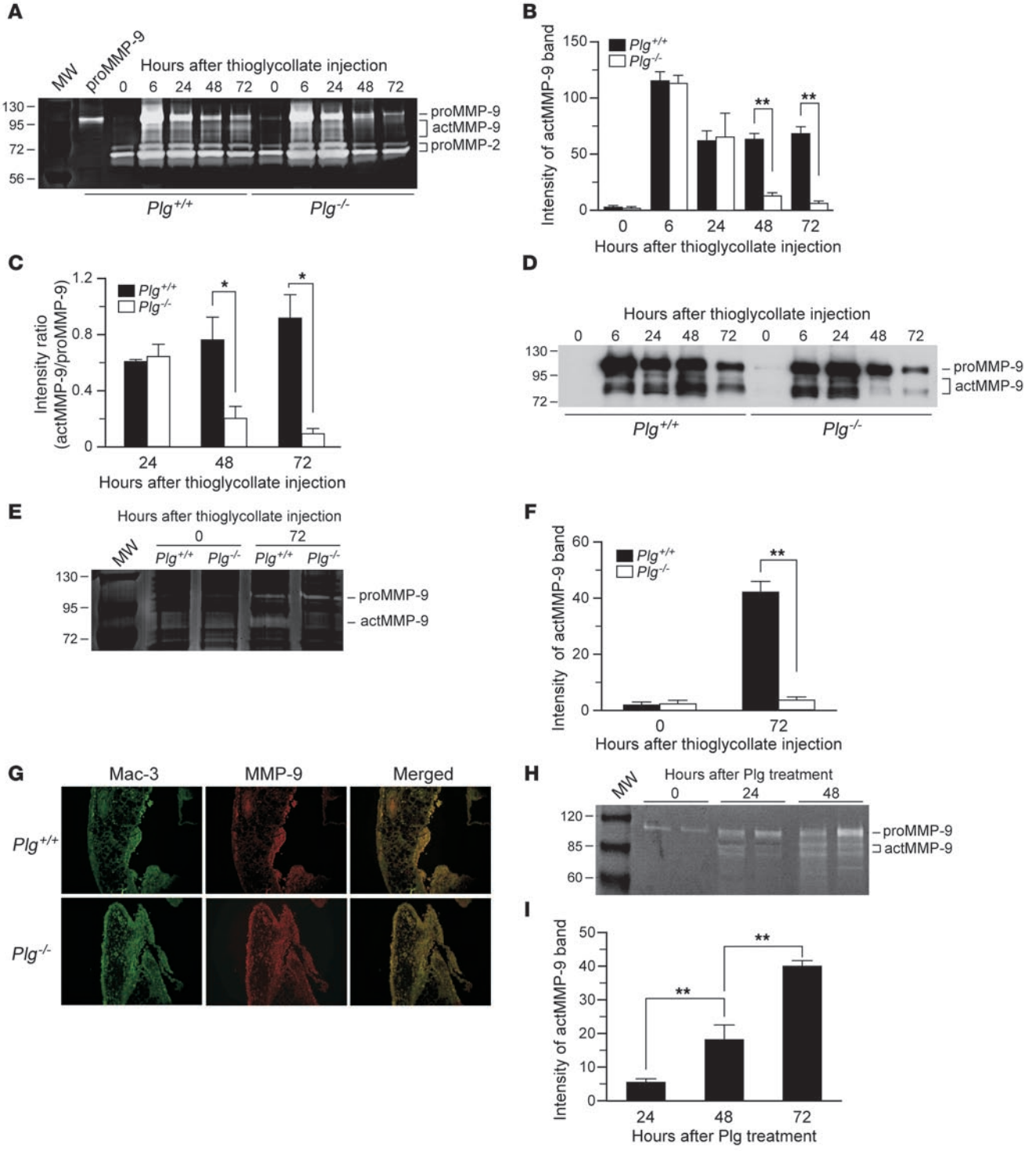

Figure 4

MMP-9 is activated by Plg in vivo and in vitro. (**A**–**D**) MMP–9 activity. PLF was collected after thioglycollate treatment at different time points and subjected to MMP-9 activity analysis. proMMP-9 (105 kDa) and actMMP-9 (95 kDa, 88 kDa), as well as proMMP-2 (72 kDa and 69 kDa), were identified by molecular weight relative to markers and purified protein. (**A**) Gelatin zymography. (**B** and **C**) Quantitation of the intensity of actMMP-9 bands and the ratio of actMMP-9 to proMMP-9 bands from zymogram results ($n = 3$). (**D**) MMP-9 immunoblot. PLF was purified by gelatin-agarose and detected with MMP-9 antibody. (**E** and **F**) Peritoneal tissue extracted and analyzed by gelatin zymography. (**E**) Gelatin zymography. (**F**) Intensity of actMMP-9 bands in peritoneal tissue ($n = 3$). (**G**) Colocalization of macrophages and MMP-9 in peritoneal tissue. Tissue sections, 72 hours after thioglycollate treatment, double immunofluorescently stained for macrophages (Mac-3 antibody, green) and MMP-9 (MMP-9 antibody, red). Original magnification, ×100. Representative images taken from 3 experiments. (**H**) Peritoneal macrophages derived from *Plg*$^{+/+}$ mice were isolated and cultured, which was followed by treatment with or without Plg (10 μg/ml) for 24 or 48 hours. The culture medium was collected and subjected to gelatin zymography. (**I**) Intensity of actMMP-9 bands in the culture medium of macrophages (3 independent assays).*$P < 0.05$, **$P < 0.01$.

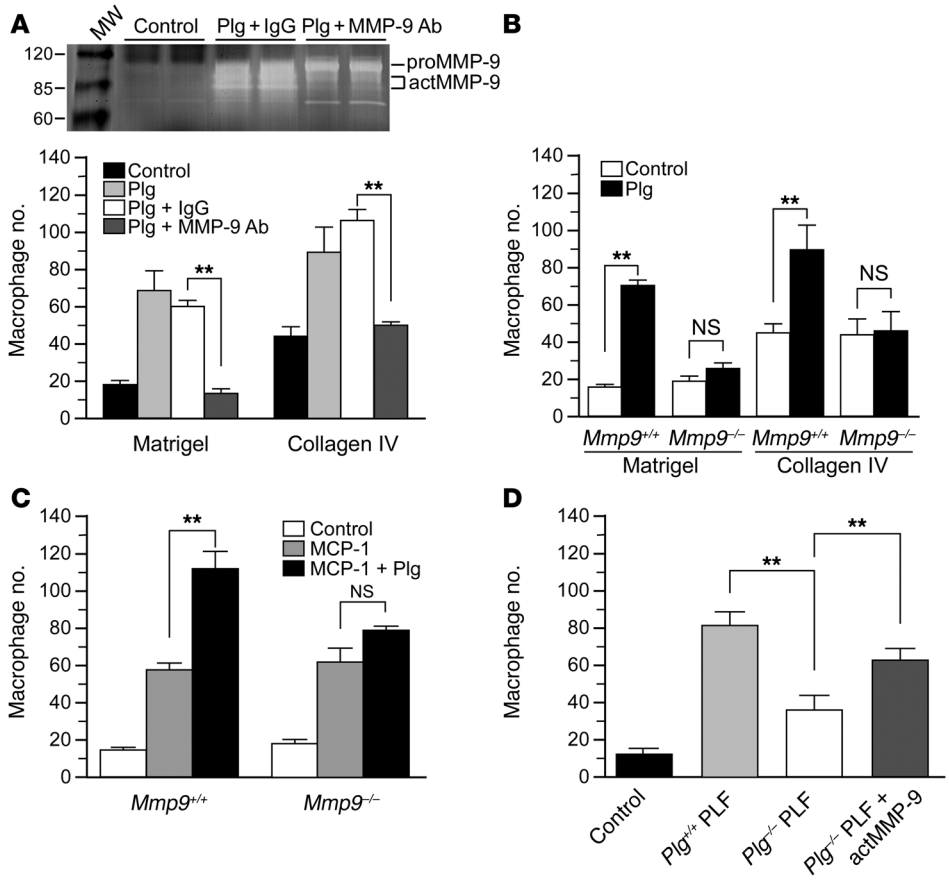

Figure 5

MMP-9 activation is required for Plg-induced macrophage migration in vitro. (**A** and **B**) Macrophage migration across Matrigel or collagen IV with serum as the chemoattractant was assayed. (**A**) MMP-9 neutralization blocks Plg-mediated macrophage migration. *Plg*$^{+/+}$ macrophage migration was determined in the presence or absence of Plg, with MMP-9 antibody or control IgG. Inset: Gelatin zymography assay for culture medium of peritoneal macrophages treated with PBS, Plg plus IgG, or Plg plus MMP-9 antibody. (**B**) MMP-9 deficiency blocks Plg-mediated macrophage migration. Migration of *Mmp9*$^{+/+}$ or *Mmp9*$^{-/-}$ macrophages was determined with or without Plg treatment. (**C**) MMP-9 knockout blocks Plg-mediated macrophage migration across Matrigel with MCP-1 as the chemoattractant. (**D**) Reconstitution of actMMP-9 restores macrophage migration in response to PLF from *Plg*$^{-/-}$ mice. The migration of *Plg*$^{+/+}$ macrophages was determined in response to PLF (chemoattractant) collected from *Plg*$^{+/+}$ and *Plg*$^{-/-}$ mice with or without actMMP-9. In **A**–**D**, "Control" indicates wells with cells and medium only. Migrated cells were counted by microscopy in 4 high-power fields for each insert (3 separate experiments performed in triplicate). $^{**}P < 0.01$.

and there was no detectable difference in the laminin content of the peritoneal tissue of *Plg*$^{+/+}$ and *Plg*$^{-/-}$ mice treated with thioglycollate. These results imply that a proteolytic mechanism responsible for degradation of the collagen IV layer during cell migration may be altered in Plg-deficient mice.

MMP-9 is activated by Plg in vivo and in vitro. MMPs are the primary proteolytic enzymes responsible for ECM remodeling (4), and Plg is known to play a role in the activation of MMPs (27). Accordingly, we investigated whether MMPs are involved in the Plg-regulated macrophage migration in the thioglycollate inflammatory model. A zymography assay was employed to assess the proteolytic activity of MMPs in PLF from thioglycollate-stimulated *Plg*$^{+/+}$ and *Plg*$^{-/-}$ mice (Figure 4A). The proenzyme form of MMP-9 (proMMP-9; 105 kDa) and the active form of MMP-9 (actMMP-9; 95 kDa, 88 kDa) were identified from molecular weight markers (28, 29). The molecular weight of unglycosylated MMP-9 shifts only about 10 kDa, while actMMP-9 shifts approximately 20 kDa (30). At time 0, prior to thioglycollate injection, inactive proMMP-9 or actMMP-9 was not detected in the PLF of either *Plg*$^{+/+}$ or *Plg*$^{-/-}$ mice. Thioglycollate induced a time-dependent MMP-9 activation in the PLF of *Plg*$^{+/+}$ and *Plg*$^{-/-}$ mice. In the *Plg*$^{+/+}$ mice, MMP-9 activity reached a peak at 6 hours and was sustained for 72 hours. However, in *Plg*$^{-/-}$ mice, a shorter duration (6–24 hours) of MMP-9 activation was observed, and there were no detectable actMMP-9 bands at 48 or 72 hours. The 2-band pattern of proMMP-2 (MW, 69 and 72 kDa) was detected at 0–72 hours, and its activity was not changed in *Plg*$^{+/+}$ or *Plg*$^{-/-}$ mice during thioglycollate stimulation (Figure 4A). This time course of MMP-9 activation was confirmed by a quantitative actMMP-9 analysis of 3 separate zymographs (Figure 4B). To rule out of the possibility that reduced MMP-9 activation may be due to fewer macrophages in the lavage of *Plg*$^{-/-}$ mice, the ratio of actMMP-9 to proMMP-9 was calculated (Figure 4C). Consistently, Plg deficiency induced a time-dependent inhibition in MMP-9 activation during thioglycollate-induced inflammation.

The activation status of MMP-9 was confirmed by subjecting the PLF to immunoblotting with an antibody that recognizes both intact (inactive) and cleaved (active) forms of MMP-9. The pattern of activation by zymography was confirmed by Western blot analysis (Figure 4D). Specifically, in *Plg*$^{+/+}$ mice, 2 peaks of activated MMP-9 were detected; one coincided with the peak of neutrophil recruitment (6–24 hours), and the second coincided with the peak macrophage accumulation (48–72 hours). Only 1 peak of activated MMP-9 occurred in *Plg*$^{-/-}$ mice at peak neutrophil accumulation (6–24 hours). actMMP-9 decreased over time in the *Plg*$^{-/-}$ mice. actMMP-9 was also reduced in the peritoneal tissue at 72 hours in the *Plg*$^{-/-}$ compared with *Plg*$^{+/+}$ mice (Figure 4, E and F). Thus, MMP-9 activation patterns correlated with the leukocyte recruitment in thioglycollate-induced peritoneal inflammation, suggesting that MMP-9 activation may play an important role in leukocyte migration in this model.

To determine the source of the MMP-9 after thioglycollate injection, tissue was immunofluorescently stained (Figure 4G) for macrophages (green) and MMP-9 (red). In agreement with the immunohistochemistry results (Figure 2A), increased peritoneal

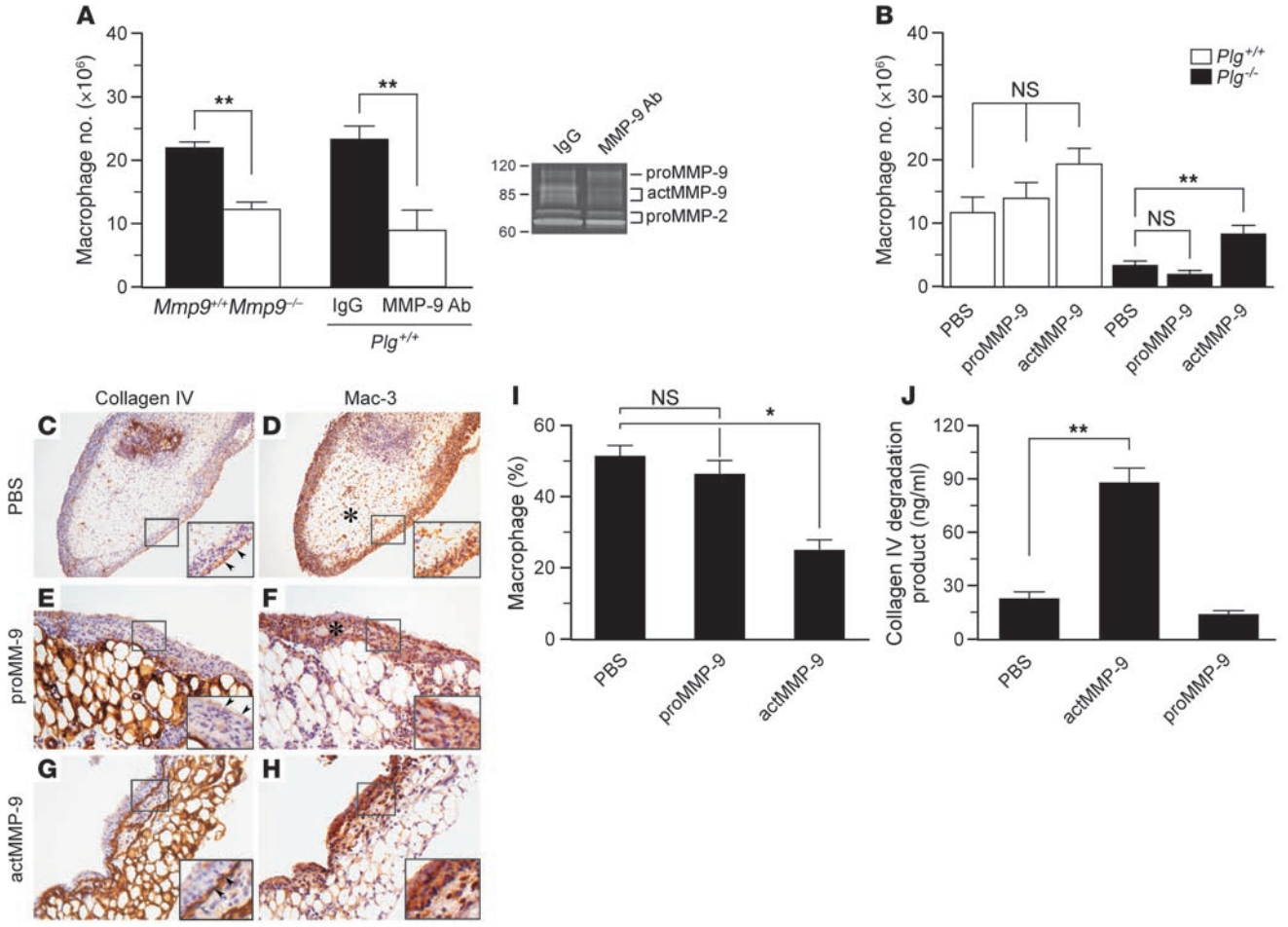

Figure 6

Macrophages require MMP-9 in vivo to migrate across peritoneal tissue, and actMMP-9 rescues impaired macrophage migration in *Plg*$^{-/-}$ mice. (**A**) Macrophage migration in *Mmp9*$^{+/+}$ or *Mmp9*$^{-/-}$ mice and in *Plg*$^{+/+}$ mice treated with control IgG or anti–MMP-9 antibody was measured 72 hours after thioglycollate injection (n = 5–7). Inset, gelatin zymograph of PLF from *Plg*$^{+/+}$ mice treated with IgG or MMP-9 antibody shows that the MMP-9 neutralization abolishes MMP-9 activation. (**B**–**J**) Before thioglycollate injection, mice were treated with PBS, proMMP-9, and actMMP-9, and 48 hours after thioglycollate injection, peritoneal lavage and tissue were collected. Results are from 3 independent assays (n = 5–7). (**B**) actMMP-9 restores the suppressed macrophage recruitment to the peritoneal cavity in *Plg*$^{-/-}$ mice. (**C**–**H**) Collagen IV (collagen IV antibody) and macrophage (Mac-3 antibody) immunostaining in *Plg*$^{-/-}$ mice. Arrowheads indicate mesothelial layer; asterisk indicates macrophage accumulation area. Original magnification (**C** and **D**), ×100; insets, ×200. Original magnification (**E**–**H**), ×200; insets, ×400. (**I**) Macrophage distribution expressed as percentage of total sample area in peritoneal tissue. (**J**) Soluble collagen IV degradation products in PLF of *Plg*$^{-/-}$ mice. *P < 0.05, **P < 0.01.

tissue macrophage accumulation was observed in *Plg*$^{-/-}$ compared with *Plg*$^{+/+}$ mice. Also, the distribution of MMP-9 was similar to that of macrophages, as indicated by their colocalization (yellow), suggesting that macrophages themselves are a main source of MMP-9 in peritoneal tissue. To verify that Plg is able to activate MMP-9 from peritoneal macrophages, MMP-9 activity was measured by gelatin zymography in Plg-treated peritoneal macrophages. Plg induced MMP-9 activation in a time-dependent fashion (Figure 4, H and I). Taken together, these data support the hypothesis that Plg facilitates macrophage migration by activating MMP-9 derived from macrophages during inflammation.

MMP-9 activation is required for Plg-induced macrophage migration in vitro. To test whether MMP-9 activation is required for the Plg-regulated macrophage migration in vitro, cell migration assays were performed with macrophages from *Plg*$^{+/+}$, *Mmp9*$^{+/+}$, and *Mmp9*$^{-/-}$ mice. The migration of the macrophages across Matrigel, a complex basement membrane model, or collagen IV was assessed in *Plg*$^{+/+}$ mice macrophages in the presence or absence of a MMP-9–neutralizing antibody or IgG as a control (Figure 5A). In separate experiments, we found that this neutralizing antibody effectively blocked plasmin-induced MMP-9 activation (Figure 5A, inset). Macrophage migration (with serum as the chemoattractant) across both Matrigel and collagen IV was enhanced by Plg. This increase in macrophage migration induced by Plg was completely abolished by MMP-9 neutralization. These results were independently corroborated using macrophages derived from *Mmp9*$^{+/+}$ and *Mmp9*$^{-/-}$ mice. Without addition of Plg (Figure 5B), migration across both substrata was similar for macrophages derived from *Mmp9*$^{+/+}$ and *Mmp9*$^{-/-}$ mice. With the addition of Plg, the migration of macrophages derived from *Mmp9*$^{+/+}$ mice was significantly increased on both Matrigel and collagen IV. In contrast, Plg had no significant affect on the migration of

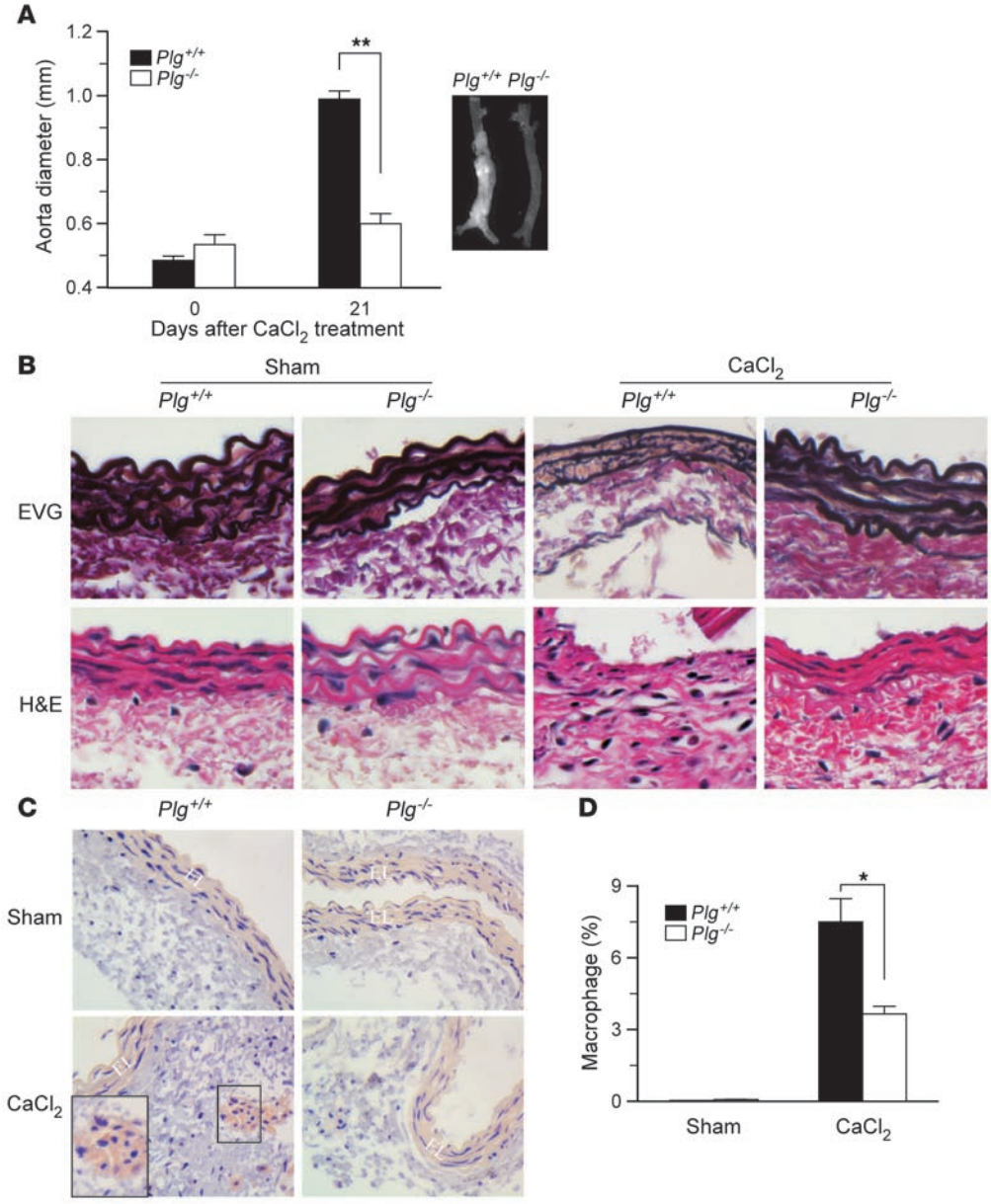

Figure 7
Prevention of AAA by Plg deficiency. Three weeks after treatment ($CaCl_2$ or NaCl), abdominal aorta was dissected and examined (n = 6–8). (**A**) Aortic diameter as measured before and after treatment (left). Representative photograph (right). (**B**) Aorta stained with EVG for elastic lamella (top row) and H&E for inflammatory cells (bottom row). Original magnification, ×400. (**C**) Macrophages (Mac-3 antibody) in aorta. EL, elastic lamellae. Original magnification, ×200; inset, ×400. (**D**) Macrophage distribution expressed as percentage of tissue area in aortic tissue (n = 4–5). $^*P < 0.05$, $^{**}P < 0.01$.

macrophages from the *Mmp9*$^{-/-}$ mice on both substrata. Similar results were observed when monocyte chemoattractant protein–1 (MCP-1) was used as a chemoattractant (Figure 5C). MCP-1 alone increased the migration of both *Mmp9*$^{+/+}$ and *Mmp9*$^{-/-}$ macrophages, but with Plg treatment, only *Mmp9*$^{+/+}$ macrophage migration had a significant additional increase (~2-fold) in response to MCP-1. Plg did not increase the migration of *Mmp9*$^{-/-}$ macrophages in response to MCP-1.

In addition, the PLF derived from thioglycollate-stimulated *Plg*$^{+/+}$ and *Plg*$^{-/-}$ mice at 72 hours was used as the chemoattractant. The PLF derived from *Plg*$^{+/+}$ mice enhanced macrophage migration across the Matrigel by 3-fold compared with the PLF from *Plg*$^{-/-}$ mice, but with actMMP-9 added to the PLF from the *Plg*$^{-/-}$ mice, macrophage migration was significantly rescued (Figure 5D). In summary, these data demonstrate an essential role of MMP-9 for Plg-induced macrophage migration across ECM in vitro.

MMP-9 activation is required for Plg-dependent macrophage but not neutrophil migration in vivo. The effects of MMP-9 deficiency or its neutralization with antibody on macrophage recruitment in the thioglycollate model were evaluated. Thioglycollate-induced macrophage recruitment in MMP-9–deficient mice (with the same C57BL/6J [B6] background as *Plg*$^{-/-}$ mice) was significantly reduced, by 44%, compared with that in *Mmp9*$^{+/+}$ mice (Figure 6A). Additionally, MMP-9 neutralization in *Plg*$^{+/+}$ mice injected with an MMP-9 antibody efficiently (by 59%) inhibited macrophage recruitment (Figure 6A). Efficient and selective blockade of MMP-9 activity was detected in PLF (Figure 6A, inset). As a negative control, MMP-9 antibody did not affect macrophage migration in *Plg*$^{-/-}$ mice ($2.6 \times 10^6 \pm 0.1 \times 10^6$ cells; n = 4) compared with *Plg*$^{-/-}$ mice plus IgG ($3.2 \times 10^6 \pm 0.2 \times 10^6$ cells; n = 3). When MMP-2–neutralizing antibody, as confirmed by zymography, was tested in *Plg*$^{+/+}$ mice, no significant effect on mac-

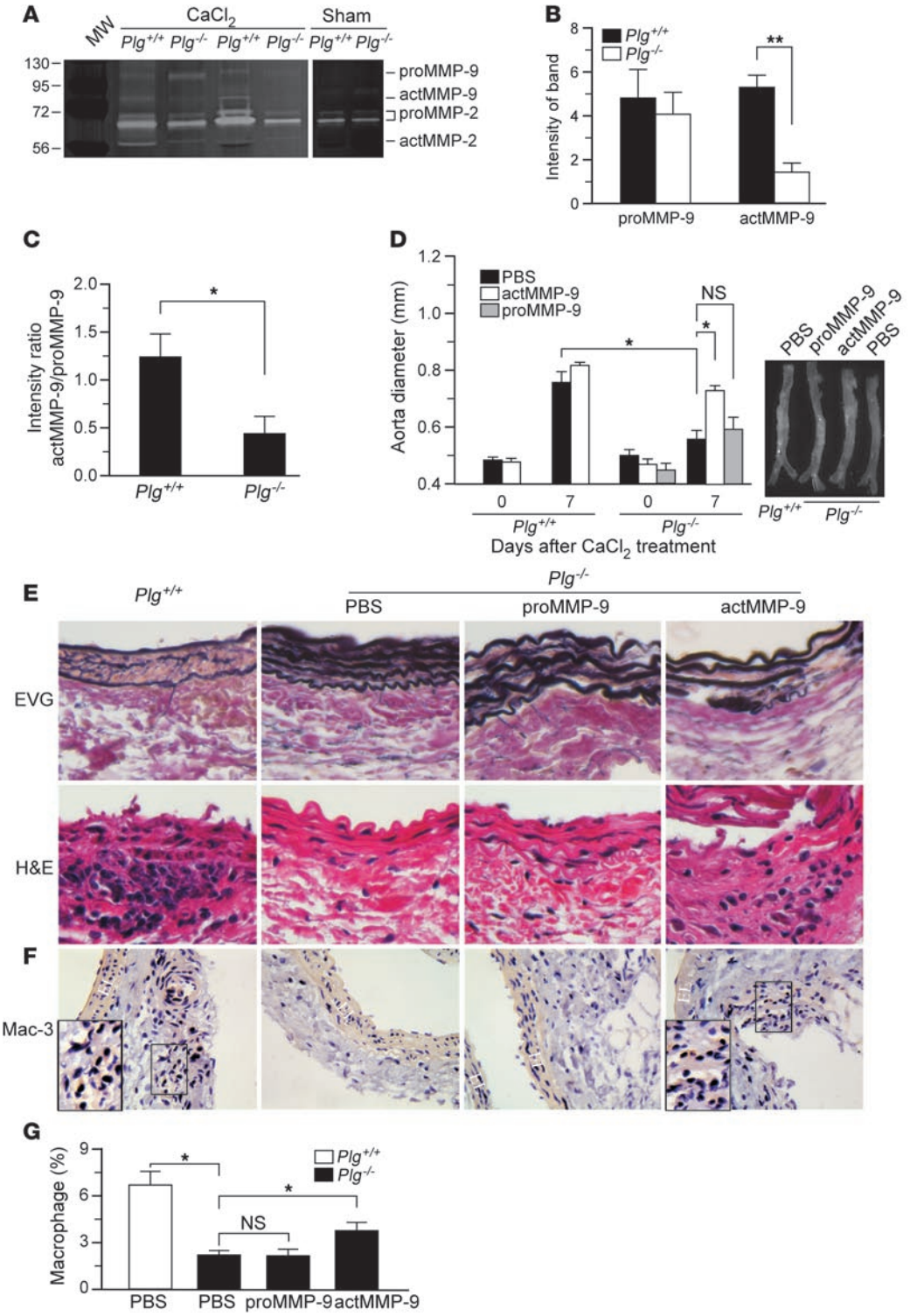

Figure 8
Plg-mediated AAA formation requires MMP-9. (**A**–**C**) MMP activity in aorta 1 week after $CaCl_2$ or NaCl (Sham) treatment. (**D**–**G**) $CaCl_2$-treated mice were injected with proMMP-9, actMMP-9, or PBS ($n = 5$–7), and 1 week after treatment, the abdominal aortas were examined. (**A**) Extracted aorta tissue (5 μg protein) was analyzed by gelatin zymography. (**B**) Intensity of actMMP-9 bands in zymogram assays (3 independent assays). (**C**) Intensity ratio (actMMP-9/proMMP-9) of zymogram assays. (**D**) Aortic diameter before and after treatment (left). Representative aortas are shown (right). (**E**) Aorta sections stained for elastic lamellae (EVG) and inflammatory cells (H&E). Original magnification, ×400. (**F**) Macrophages (Mac-3 antibody). Original magnification, ×200; insets, ×400. (**G**) Macrophage distribution expressed as percentage of total sample area in aorta ($n = 4$–5). $^*P < 0.05$, $^{**}P < 0.01$.

rophage migration (IgG, $15.2 \times 10^6 \pm 1.0 \times 10^6$ cells; MMP-2 antibody, $12.7 \times 10^6 \pm 2.6 \times 10^6$ cells) was detected. In other parallel studies, both MMP-9 deficiency and MMP-9 neutralization failed to inhibit thioglycollate-induced neutrophil migration (data not shown). Thus, in the thioglycollate-induced inflammation model, MMP-9 is required for migration of macrophages but not neutrophils.

To test whether MMP-9 activation is necessary for Plg-regulated macrophage migration, *Plg*$^{-/-}$ mice were injected with actMMP-9 or proMMP-9 before and during the thioglycollate-induced inflammation. The number of recruited macrophages was restored to a significant extent (by 57%) in *Plg*$^{-/-}$ mice treated with actMMP-9 at either 50 μg/kg per injection (Figure 6B) or 100 μg/kg per injection ($10.9 \times 10^6 \pm 0.7 \times 10^6$ cells; $n = 4$). proMMP-9 was not able

to restore the macrophage migration. Neither proMMP-9 nor actMMP-9 significantly enhanced macrophage recruitment in $Plg^{+/+}$ mice. Treatment with actMMP-2 was unable to reverse the Plg deficiency–inhibited macrophage recruitment ($1.63 \times 10^6 \pm 0.2 \times 10^6$ cells; $n = 4$) to the PLF.

There were major differences in collagen and macrophage distribution in sections of peritoneal tissue from $Plg^{-/-}$ mice treated with PBS or proMMP-9 compared with the actMMP-9–treated $Plg^{-/-}$ mice (Figure 6, C–H). In the PBS- and proMMP-9–treated mice, collagen IV in the mesothelial layer remained intact and macrophage migration across the mesothelial layer was impeded, resulting in accumulation of macrophages in submesothelial layer and decreased accumulation of cells in the cavity side of the layer. With actMMP-9 treatment, the collagen IV layer was discontinuous, and macrophages successfully migrated out of collagen IV layer in mesothelium, suggesting that actMMP-9 degradation of collagen IV rescued macrophage migration in $Plg^{-/-}$ mice. Quantitatively, actMMP-9 treatment significantly reduced macrophage accumulation in the submesothelial layer (Figure 6I). Furthermore, a 2-fold increase in collagen IV degradation, as indicated by increased fragmented collagen IV in the PLF, was detected in actMMP-9–treated $Plg^{-/-}$ mice (Figure 6J). These data suggest that the activation of MMP-9 is required for Plg-regulated macrophage migration in the thioglycollate model.

AAA development is prevented by Plg deficiency. Macrophage-mediated MMP activation is crucial for the development of AAA (31). To test whether Plg-regulated MMP-9 activation is required for AAA progression, we first determined whether Plg is required for the aneurysm development in a mouse AAA model induced by periaortic application of $CaCl_2$. The $CaCl_2$-induced AAA model is a widely used model to study AAA (32–34). A major advantage of using the $CaCl_2$ model is the rapid formation of the aneurysm. This model is better suited for the $Plg^{-/-}$ mice, where long-term development of disease is impractical due to the deterioration of their health. Three weeks after treatment, there was no significant change in aortic diameter or morphology in $Plg^{-/-}$ mice, compared with that before treatment (Figure 7A). However, in $Plg^{+/+}$ mice, there was a 2-fold increase in aortic diameter after $CaCl_2$ treatment. Surgery (sham operation) itself did not alter aortic diameter (data not shown) or morphology in either background. In elastica van Gieson–stained sections, the elastic lamellae were normal in $CaCl_2$-treated $Plg^{-/-}$ mice, similar to those in sham-operated mice, while disruption and fragmentation of elastic lamellae were observed in $Plg^{+/+}$ mice treated with $CaCl_2$ (Figure 7B, top row).

Infiltration of inflammatory cells was greater in the media and adventitia of aorta from $Plg^{+/+}$ mice than from $Plg^{-/-}$ mice treated with $CaCl_2$ (Figure 7B, bottom row). To investigate the involvement of macrophages in aneurysm progression, macrophages were immunostained with Mac-3. $CaCl_2$-treated $Plg^{-/-}$ mice had remarkably fewer macrophages in the media and adventitia compared with $Plg^{+/+}$ mice, and no macrophages were observed in sham-operated mice (Figure 7C). In Plg-deficient mice, macrophage infiltration was reduced by half in the media and adventitia compared with that in $Plg^{+/+}$ mice (Figure 7D). These data indicate that Plg is required for the pathological progression, including elastin degradation and macrophage recruitment, during AAA development.

Plg-mediated AAA formation requires MMP-9. To determine the role of MMPs in Plg-mediated AAA development, protease activity in aneurysm tissue was examined by gelatin zymography. Compared with sham operation, $CaCl_2$ treatment induced both MMP-9 and MMP-2 activation in $Plg^{+/+}$ mice (Figure 8A). In $Plg^{-/-}$ mice, the MMP-9 protease activity in the aneurysm tissues (Figure 8, A–C) was diminished by 80% and MMP-2 activity was reduced by 82% (band intensity, 0.5 ± 0.1) compared with that in $Plg^{+/+}$ mice (band intensity, 2.7 ± 0.6). However, MMP-12, another MMP associated with aneurysm formation, was not quantitatively different in $Plg^{+/+}$ and $Plg^{-/-}$ mice in this model (Supplemental Figure 2; supplemental material available online with this article; doi:10.1172/JCI32750DS1). When $Plg^{-/-}$ mice were treated with actMMP-9, dilation of aortic diameter increased significantly (1.5-fold), while administration of proMMP-9 failed to induce a significant effect (Figure 8D). Administration of actMMP-9 to the aorta effectively increased actMMP-9 in aorta in the $Plg^{-/-}$ mice (data not shown). Furthermore, treatment with actMMP-9 induced disruption and fragmentation of elastic lamellae in $Plg^{-/-}$ AAA mice, similar to the pathological features in the aneurysms in $Plg^{+/+}$ mice (Figure 8E, top row). In comparison, leukocyte infiltration into the media and adventitia was accompanied by disruption of the elastic lamellae in $Plg^{+/+}$ and actMMP-9–treated $Plg^{-/-}$ mice but not PBS- or proMMP-9–treated mice (Figure 8E, bottom row). Macrophage recruitment to the media and adventitia was verified by immunohistochemical staining (Figure 8F). Treatment with actMMP-9 induced a significant increase in macrophage recruitment into the aneurysm tissue in $Plg^{-/-}$ mice compared with that observed in proMMP-9–treated $Plg^{-/-}$ mice (Figure 8G). These data establish an essential role of MMP-9 activation in Plg-mediated AAA development.

Discussion

The mechanism of Plg-dependent inflammatory cell recruitment was investigated in 2 models: thioglycollate-induced peritonitis and AAA, an atherosclerotic and inflammatory model. Our study provides in vivo evidence that Plg/plasmin is required for macrophage recruitment and this role is mediated through activation of MMP-9. These conclusions are based on the following results: (a) Plg deficiency markedly reduced macrophage recruitment in both models; (b) suppressed macrophage recruitment with unaffected monocyte blood level is due to macrophage accumulation in tissue in the thioglycollate model; (c) in the thioglycollate model, macrophage migration in vivo is consistent with the time course of activation of the primary proteolytic enzyme for collagen, MMP-9; (d) $Plg^{-/-}$ mice are protected from AAA formation; (e) macrophage infiltration and MMP-9 activity in the aorta are reduced in $Plg^{-/-}$ mice; and (f) actMMP-9 restored macrophage migration in $Plg^{-/-}$ mice in both models. These data establish that Plg-dependent macrophage migration results from Plg's activation of MMP-9, which regulates the ability of inflammatory cells to invade ECM at sites of injury.

Trans-ECM migration is an important step in leukocyte migration. In the thioglycollate model, the collagen IV layer beneath the mesothelial cells acted as a barrier for macrophage emigration into the peritoneal cavity. In this model, Plg-dependent macrophage migration required MMP-9 activation and degradation of collagen IV. Other studies have also demonstrated that MMP-9–induced collage IV degradation is important for cell migration (35–37). Although MMP-9 is not an interstitial collagenase, MMP-9 may participate in the degradation of interstitial collagen indirectly. Recent studies suggested that cleaved fragments of several matrixes (substrates of MMP-9) and MMP-9–activated cytokines were able to induce interstitial collagenases expression (38–40). Also, MMP-9 may work in concert with other MMPs to degrade interstitial collagens. Therefore, MMP-9 may not be sufficient but is

necessary for the Plg-regulated macrophage migration. In aorta, both elastin (a substrate of MMP-9) and interstitial collagen are important ECM components. During aneurysm formation, elastin degradation is thought to initiate aorta dilation, while loss of fibrillar collagen predisposes to aneurysm rupture (8). Our data establish a mechanism (Plg/MMP-9) for the initiation and formation of aneurysm. In our $CaCl_2$-induced aneurysm model, rupture does not occur, so it remains to be determined whether Plg regulates degradation of interstitial collagens to induce rupture in the late phase of aneurysm progression.

Macrophage migration in *Mmp9*$^{-/-}$ mice is slightly higher than in *Plg*$^{-/-}$ mice, leading us to investigate whether other MMPs are involved in macrophage migration in the thioglycollate model. *Mmp9*$^{+/+}$ and *Mmp9*$^{-/-}$ mice stimulated with thioglycollate were treated with galardin (41), a broad-spectrum MMP inhibitor. Galardin injection (Supplemental Figure 1) resulted in a reduction in macrophage migration in *Mmp9*$^{-/-}$ mice, suggesting the potential involvement of other MMPs in macrophage recruitment. Given that Plg treatment is unable to increase the migration of *Mmp9*$^{-/-}$ macrophages in vitro and that administration of actMMP-9 efficiently restores the macrophage migration suppressed by Plg deficiency in vitro and in vivo, other MMPs (not MMP-9) involved in the macrophage migration in peritonitis may be limited to non–Plg-mediated events during cell migration. This hypothesis is also supported by our data showing that MMP-9 deficiency fails to alter macrophage migration induced by MCP-1, indicating that the effect of MMP-9 on macrophage migration was independent of MCP-1–mediated macrophage migration.

The outcomes of studies designed to determine whether Plg activators (uPA and tPA) are required for macrophage migration have been variable, and this variation may depend on several factors, including the background of gene-targeted mice or the inflammatory model (13, 42–45). In the thioglycollate model, reduced macrophage migration is found in uPA-deficient mice in a B6 background but not in a mixed (B6 × 129) background (J. Hoover-Plow, unpublished observations). These inconsistencies may be due in part to the marked difference in macrophage migration in B6 and 129 mice in the thioglycollate model (46). However, uPA rather than tPA plays the dominant role in macrophage infiltration in vascular injury models including AAA (15–19), which implies that Plg may be involved in AAA development. However, uPA has been reported to induce leukocyte adhesion and migration as well as expression of MMPs independent of its role in the activation of Plg (43). By using *Plg*$^{-/-}$ mice, our study provides direct evidence that Plg-mediated MMP-9 activation is required for macrophage migration and AAA formation.

Studies have reported conflicting results regarding the dependence of macrophage infiltration on MMP-9 using *Mmp9*$^{-/-}$ mice. Luttun et al. (7) and Choi et al. (47) reported fewer tissue macrophages in atherosclerosis lesion in *Apoe*$^{-/-}$*Mmp9*$^{-/-}$ mice, while Pyo et al. (48) and Longo et al. (33) reported that although MMP-9 deficiency protected against aneurysm formation, macrophage infiltration into aortas was not impaired in *Mmp9*$^{-/-}$ mice. Our results showed that in $CaCl_2$-induced AAA model, Plg-mediated MMP-9 activation is responsible for macrophage infiltration into aorta. There are 2 possible explanations for these discrepancies: first, the background of *Mmp9*$^{-/-}$ mice is different among these studies, and our own work (46) as well as that of others (49, 50) shows that genetic background influences inflammatory responses; and second, Longo et al. (33) suggested that MMP-2 and MMP-9 work in concert to produce AAA. MMP-2 expression was higher in *Mmp9*$^{-/-}$ mice (51) and may maintain the macrophage infiltration to the aorta in *Mmp9*$^{-/-}$ mice, while in *Plg*$^{-/-}$ mice, activation of both MMP-9 and MMP-2 is inhibited, resulting in blockage of macrophage infiltration in AAA.

In summary, our findings demonstrate that MMP-9 activation by Plg is crucial to the Plg-dependent regulation of macrophage trans-ECM migration in inflammation and development of AAA. Targeting the Plg/MMP-9 pathway may offer a new approach for therapeutic intervention in inflammation-associated CVD.

Methods

Mice. The Plg-deficient mice were previously generated and backcrossed into the B6 background (12). The Plg-heterozygous mice were bred and offspring genotyped by PCR as previously described (52). *Mmp9*$^{-/-}$ mice in a B6 background were generously provided by Robert Senior, Washington University in St. Louis, St. Louis, Missouri, and Robert Fairchild of the Cleveland Clinic Lerner Research Institute. Mice were bred, housed in sterilized isolator cages, maintained on a 14-hour light/10-hour dark cycle, and provided with sterilized food and water ad libitum at the Biological Resource Unit of the Cleveland Clinic Lerner Research Institute. Both male and female *Plg*$^{+/+}$ and *Plg*$^{-/-}$ mice were tested between 6 and 9 weeks of age. All animal experiments were performed in accordance with protocols approved by the Institutional Animal Research Committee.

Peritoneal inflammatory model. Mice were injected i.p. with thioglycollate, 0.5 ml of 4% thioglycollate (BD Biosciences — Pharmingen), or saline (control, indicated as 0 hours), and at different times (6, 24, 48, or 72 hours), 4 ml PBS was injected into peritoneal cavity and 2.5 ml lavage was collected. Peritoneal tissue was dissected for histologic studies. The peritoneal lavage was centrifuged and the supernatant solution collected as PLF, and cells were subjected to enzyme activity assays described previously (11) to determine number of neutrophils and macrophages. To determine the origin of the macrophages, leukocytes were labeled in vivo with PKH2-PCL, a fluorescent dye that is selectively phagocytized and thereby labels monocytes and neutrophils. The dye is nontoxic; nonphagocytized dye disappears by 24 hours; and the dye persists in vivo in the cells for more than 21 days (23). PKH2-PCL (Sigma-Aldrich) (0.1 ml of 50 μM per mouse) was administrated to mice by tail vein injection 24 hours before thioglycollate injection. At 72 hours after the thioglycollate injection, peritoneal cells were collected and centrifuged to slides (Shandon Cytospin 3; Thermo Scientific) (10^5 cells/slide). The percentage of PKH2-PCL–labeled cells was determined by counting the number of fluorescently labeled cells by fluorescence microscopy and counting the total number of cells by light microscopy (3 random fields, ×200 magnification). The slides also were stained with Wright's stain, and the percentage of macrophages was determined by differentiation counting. Finally, the percentage of PKH2-labeled macrophages (blood-derived macrophages) was calculated by correcting the percentage of fluorescently labeled cells with the percentage of macrophages. Experiments were preformed in duplicate and the mean of 3 mice per genotype calculated.

Drug administration in peritoneal inflammation model. Tranexamic acid (Sigma-Aldrich) was administrated in the drinking water at 20 mg/ml 48 hours prior to thioglycollate injection and throughout the experiment or 0.5 mg aprotinin injected daily before and after thioglycollate injection. The mice treated with tranexamic acid or aprotinin showed no overt adverse reaction to the drugs. Mice were administered, by i.p. injection, mouse proMMP-9 (50 μg/kg body weight; PF068; Calbiochem, EMD Biosciences) or human actMMP-9 (50 or 100 μg/kg; PF140; Calbiochem, EMD Biosciences) 1 hour prior to the injection of thioglycollate and then twice daily. For MMP-9 neutralization experiments, MMP-9–neutralizing antibody (4 mg/kg; IM09L; Calbiochem, EMD Biosciences) or control mouse IgG (4 mg/kg; Jackson

ImmunoResearch Laboratories Inc.) was injected (i.p.) into mice twice, 2 hours before and 24 hours after the thioglycollate injection.

AAA model. AAA was induced by periaortic application of $CaCl_2$ (53). Mice at age approximately 6–8 weeks were anesthetized (80 mg/kg ketamine/5 mg/kg xylazine) and the abdominal aorta between the renal arteries and bifurcation of the iliac arteries was isolated from surrounding tissue. An image of the aorta was acquired by SPOT imaging software version 4.0.3 (Diagnostic Instruments Inc.) through a cooled CCD camera attached to the Olympus SZ-PT dissection microscope. After image acquisition, cotton gauze (1 × 0.5 cm) that had been soaked in 0.5 M $CaCl_2$ solution was applied to the external surface of the aorta. NaCl (0.9%) was substituted for $CaCl_2$ in sham-operated mice. After 10 minutes, the aorta was rinsed with 0.9% sterile saline and the incision was closed. In some experiments, after $CaCl_2$ treatment, PBS, proMMP-9 (2 μg in 5 μl PBS), or actMMP-9 (2 μg in 5 μl PBS) was applied to the aorta for 30 minutes, and then the incision was closed. For the next 3 days, these mice were injected with PBS or proMMP-9 (100 μg/kg) or actMMP-9 (100 μg/kg) intravenously by tail vein. Either 1 or 3 weeks later, mice were anesthetized and the aorta exposed after the surrounding fatty tissue and scarring adhesions were dissected away. After image acquisition, the mice were euthanized, and the aortas were collected for zymographic and histological analysis.

Histochemistry, immunohistochemistry, and immunofluorescence staining. Peritoneal tissue or aorta was fixed and embedded in paraffin. For peritoneal tissue, the sections (8 μm) were stained with H&E for histochemical examination or with Masson's trichrome for collagen content. Other paraffin sections were deparaffinized and blocked with 3% normal goat serum and incubated with antibodies against Mac-3 (550292; BD), mouse neutrophils (CL8993AP; Cedarlane Laboratories Ltd.), type IV collagen (AB756P; Chemicon, Millipore), laminin (AB2034; Chemicon, Millipore), or normal IgG (as control) at 4°C overnight. Subsequently, a peroxidase DAB detection system (PK6101; Vector Laboratories) was applied according to the manufacturer's instructions. Sections were counterstained with hematoxylin. For aorta tissue, the sections (5 μm thick) were stained with H&E for histochemical examination or with elastica van Gieson for elastic fiber detection. Other aorta paraffin sections were immunohistochemically stained to identify macrophages (Mac-3 antibody). The data were quantified using computer-assisted image analysis software Image-Pro Plus (Media Cybernetics). For double immunofluorescence staining, peritoneal tissue sections were stained with Mac-3 antibody (1:10), Alexa Fluor 488–conjugated goat anti-rat IgG (1:200), rabbit anti–MMP-9 antibody (1:100; AB19016; Chemicon, Millipore), and Alexa Fluor 568–conjugated goat anti-rabbit IgG (1:200). The sections were observed under a fluorescence microscope.

Plg and plasmin activity. Plg in the plasma was determined according to the method of Lijnen et al. (54). To measure plasmin activity, PLF was collected at 0–72 hours after thioglycollate injection and analyzed by electrophoresis with 10% prestained casein zymogram gels (Invitrogen). After the gels were renatured and developed according to the manufacturer's instructions, intensity of the caseinolytic bands was quantified using Kodak image analysis software (1D 3.6).

Gelatin zymography. Protease activities in the PLF, peritoneal tissue, aorta, and macrophage-conditioned medium were examined by gelatin zymography. PLF was collected following the procedure described above. Peritoneal tissue or aortic proteins were extracted (55) and protein concentration measured by BCA protein assay (Bio-Rad). Macrophages were isolated from $Plg^{+/+}$ mice 72 hours after thioglycollate injection and cultured in 6-well plates at 1×10^6/well density in 1 ml DMEM medium supplemented with 1% BSA. Macrophages were treated with Plg (20 μg/ml) for 24 or 48 hours. The same loading volume (PLF and macrophage-conditioned medium) or same amount of proteins (aorta and peritoneal tissue) were subjected to electrophoresis with 10% gelatin zymogram gels (Invitrogen). After renaturing and developing the gels according to manufacturer's instructions, the gels were stained with GelCode Blue Stain Reagent (Pierce, Thermo Scientific). The intensities of bands were quantified using ImageJ software (http://rsbweb.nih.gov/ij/).

Immunoblotting of MMP-9. MMP-9 in the PLF was isolated by gelatin-agarose as described previously (56). Samples were subjected to 4%–20% SDS-PAGE electrophoresis. After protein transfer, the PDVF membranes were blocked and incubated with anti–MMP-9 antibody (1:1,000). The signals were amplified with an ABC peroxidase detection system (PK6101; Vector Laboratories) according to manufacturer's instructions and visualized with enhanced chemiluminescence reagents (Amersham Biosciences, GE Healthcare).

Mouse collagen IV soluble fragment ELISA. Mouse collagen IV soluble fragments in PLF were measured by a competitive ELISA kit (Collagen IV M kit; Exocell). PLF (2.5 ml) was concentrated into 240 μl and collagen IV degradation products determined according to the manufacturer's instructions.

In vitro macrophage migration through ECMs. Peritoneal macrophages were harvested from $Plg^{+/+}$, $Mmp9^{+/+}$, or $Mmp9^{-/-}$ mice 72 hours after the injection of thioglycollate. The cells were washed with PBS and suspended in 0.1% BSA/DMEM medium. About 95% of the cells were macrophages identified by Wright's staining, and the viability was greater than 95%, as assessed by trypan blue staining. Migration assays were performed in 24-well chambers with inserts (8-μm pores) coated with Matrigel (354480; BD) or type IV collagen (4 μg/well). Macrophage suspension with 5×10^5 (Matrigel-coated inserts) or 2.5×10^5 cells (collagen IV–coated inserts) was added to the upper chamber. Cells were allowed to attach for 2–3 hours, and unattached cells were removed by thorough washing with PBS. The plates were incubated at 37°C for 48 hours (Matrigel-coated inserts) or 20 hours (collagen IV–coated inserts). Medium with serum (10% FBS) or MCP-1 (479-JE; R&D Systems) was added into lower chamber as a chemoattractant. Mouse Plg (10 μg/ml), isolated by a lysine-sepharose column, was added to the upper chamber, and MMP-9–neutralizing antibody (20 μg/ml) or mouse IgG (20 μg/ml) was added to both upper and lower chambers. For macrophage migration in response to PLF, $Plg^{+/+}$ or $Plg^{-/-}$ PLF (100 μl) was added to both upper and lower chambers, and actMMP-9 (2 μg/ml) was added to the upper chambers. After removal of the nonmigrating cells from the upper surface of the matrix membrane, the membrane was fixed and stained with 1% toluidine blue (Sigma-Aldrich). The number of cells that migrated completely through the 8-μm pores was determined in 4 random high-power fields (×400) for each filter. The migration assays were performed in triplicate in 3 separate experiments.

Statistics. All data in the text and figures are expressed as mean ± SEM and were analyzed using a 2-tailed *t* test. A *P* value of less than 0.05 was considered significant.

Acknowledgments

The authors thank Edward Plow for his helpful discussions and Nadine Klimczak for assistance with manuscript preparation. This study was supported by grants from the NIH: HL65205 (to J. Hoover-Plow), HL078701 (to J. Hoover-Plow), HL17964 (to J. Hoover-Plow), and T32 HL07914 (to A. Shchurin); and the American Heart Association: 0625331B (to Y. Gong).

Received for publication May 21, 2007, and accepted in revised form June 18, 2008.

Address correspondence to: Jane Hoover-Plow, Department of Molecular Cardiology, NB50, Cleveland Clinic Lerner Research Institute, 9500 Euclid Avenue, Cleveland, Ohio 44195, USA. Phone: (216) 445-8207; Fax: (216) 444-9263; E-mail: hooverj@ccf.org.

Aleksey Shchurin's present address is: Oakwood Healthcare System, Medical Education and Internal Medicine, Dearborn, Michigan, USA.

1. Stoll, G., and Bendszus, M. 2006. Inflammation and atherosclerosis: novel insights into plaque formation and destabilization. *Stroke.* **37**:1923–1932.
2. Worthylake, R.A., and Burridge, K. 2001. Leukocyte transendothelial migration: orchestrating the underlying molecular machinery. *Curr. Opin. Cell Biol.* **13**:569–577.
3. Page-McCaw, A., Ewald, A.J., and Werb, Z. 2007. Matrix metalloproteinases and the regulation of tissue remodelling. *Nat. Rev. Mol. Cell Biol.* **8**:221–233.
4. Stamenkovic, I. 2003. Extracellular matrix remodelling: the role of matrix metalloproteinases. *J. Pathol.* **200**:448–464.
5. Anidjar, S., Dobrin, P.B., Eichorst, M., Graham, G.P., and Chejfec, G. 1992. Correlation of inflammatory infiltrate with the enlargement of experimental aortic aneurysms. *J. Vasc. Surg.* **16**:139–147.
6. Shimizu, K., Mitchell, R.N., and Libby, P. 2006. Inflammation and cellular immune responses in abdominal aortic aneurysms. *Arterioscler. Thromb. Vasc. Biol.* **26**:987–994.
7. Luttun, A., and Carmeliet, P. 2001. Genetic studies on the role of proteinases and growth factors in atherosclerosis and aneurysm formation. *Ann. N. Y. Acad. Sci.* **947**:124–132.
8. Carmeliet, P. 2000. Proteinases in cardiovascular aneurysms and rupture: targets for therapy? *J. Clin. Invest.* **105**:1519–1520.
9. Zhang, L., et al. 2002. Plasminogen has a broad extrahepatic distribution. *Thromb. Haemost.* **87**:493–501.
10. Wang, N., Zhang, L., Miles, L., and Hoover-Plow, J. 2004. Plasminogen regulates pro-opiomelanocortin processing. *J. Thromb. Haemost.* **2**:785–796.
11. Busuttil, S.J., et al. 2004. A central role for plasminogen in the inflammatory response to biomaterials. *J. Thromb. Haemost.* **2**:1798–1805.
12. Ploplis, V.A., French, E.L., Carmeliet, P., Collen, D., and Plow, E.F. 1998. Plasminogen deficiency differentially affects recruitment of inflammatory cell populations in mice. *Blood.* **91**:2005–2009.
13. Ling, C., et al. 2006. Disruption of tissue plasminogen activator gene reduces macrophage migration. *Biochem. Biophys. Res. Commun.* **349**:906–912.
14. Liu, Z., et al. 2005. Synergy between a plasminogen cascade and MMP-9 in autoimmune disease. *J. Clin. Invest.* **115**:879–887.
15. Moons, L., et al. 1998. Reduced transplant arteriosclerosis in plasminogen-deficient mice. *J. Clin. Invest.* **102**:1788–1797.
16. Creemers, E., et al. 2000. Disruption of the plasminogen gene in mice abolishes wound healing after myocardial infarction. *Am. J. Pathol.* **156**:1865–1873.
17. Carmeliet, P., et al. 1997. Urokinase-generated plasmin activates matrix metalloproteinases during aneurysm formation. *Nat. Genet.* **17**:439–444.
18. Deng, G.G., et al. 2003. Urokinase-type plasminogen activator plays a critical role in angiotensin II-induced abdominal aortic aneurysm. *Circ. Res.* **92**:510–517.
19. Wang, Y.X., et al. 2001. Angiotensin II increases urokinase-type plasminogen activator expression and induces aneurysm in the abdominal aorta of apolipoprotein E-deficient mice. *Am. J. Pathol.* **159**:1455–1464.
20. Qian, H.S., et al. 2007. Overexpression of PAI-1 prevents the development of abdominal aortic aneurysm in mice. *Gene Ther.* **15**:224–232.
21. Moser, T.L., Enghild, J.J., Pizzo, S.V., and Stack, M.S. 1993. The extracellular matrix proteins laminin and fibronectin contain binding domains for human plasminogen and tissue plasminogen activator. *J. Biol. Chem.* **268**:18917–18923.
22. Lijnen, H.R. 2001. Plasmin and matrix metalloproteinases in vascular remodeling. *Thromb. Haemost.* **86**:324–333.
23. Melnicoff, M.J., Horan, P.K., and Morahan, P.S. 1989. Kinetics of changes in peritoneal cell populations following acute inflammation. *Cell. Immunol.* **118**:178–191.
24. van Furth, R., Diesselhoff-Den Dulk, M.M.C., and Mattie, H. 1973. Quantitative study on the production and kinetics of mononuclear phagocytes during an acute inflammatory reaction. *J. Exp. Med.* **138**:1314–1330.
25. Margetts, P.J., et al. 2002. Inflammatory cytokines, angiogenesis, and fibrosis in the rat peritoneum. *Am. J. Pathol.* **160**:2285–2294.
26. Nagy, J.A. 1996. Peritoneal membrane morphology and function. *Kidney Int. Suppl.* **56**:S2–S11.
27. Lijnen, H.R., et al. 1998. Function of the plasminogen/plasmin and matrix metalloproteinase systems after vascular injury in mice with targeted inactivation of fibrinolytic system genes. *Arterioscler. Thromb. Vasc. Biol.* **18**:1035–1045.
28. Ramos-DeSimone, N., et al. 1999. Activation of matrix metalloproteinase-9 (MMP-9) via a converging plasmin/stromelysin-1 cascade enhances tumor cell invasion. *J. Biol. Chem.* **274**:13066–13076.
29. Toth, M., et al. 2003. Pro-MMP-9 activation by the MT1-MMP/MMP-2 axis and MMP-3: role of TIMP-2 and plasma membranes. *Biochem. Biophys. Res. Commun.* **308**:386–395.
30. Masure, S., Nys, G., Fiten, P., Van, D.J., and Opdenakker, G. 1993. Mouse gelatinase B. cDNA cloning, regulation of expression and glycosylation in WEHI-3 macrophages and gene organisation. *Eur. J. Biochem.* **218**:129–141.
31. Shah, P.K. 1997. Inflammation, metalloproteinases, and increased proteolysis: an emerging pathophysiological paradigm in aortic aneurysm. *Circulation.* **96**:2115–2117.
32. Basalyga, D.M., et al. 2004. Elastin degradation and calcification in an abdominal aorta injury model: role of matrix metalloproteinases. *Circulation.* **110**:3480–3487.
33. Longo, G.M., et al. 2002. Matrix metalloproteinases 2 and 9 work in concert to produce aortic aneurysms. *J. Clin. Invest.* **110**:625–632.
34. Yoshimura, K., et al. 2005. Regression of abdominal aortic aneurysm by inhibition of c-Jun N-terminal kinase. *Nat. Med.* **11**:1330–1338.
35. Legrand, C., et al. 1999. Airway epithelial cell migration dynamics. MMP-9 role in cell-extracellular matrix remodeling. *J. Cell Biol.* **146**:517–529.
36. Johnson, C., and Galis, Z.S. 2004. Matrix metalloproteinase-2 and -9 differentially regulate smooth muscle cell migration and cell-mediated collagen organization. *Arterioscler. Thromb. Vasc. Biol.* **24**:54–60.
37. Bergers, G., et al. 2000. Matrix metalloproteinase-9 triggers the angiogenic switch during carcinogenesis. *Nat. Cell Biol.* **2**:737–744.
38. Yasuda, T., and Poole, A.R. 2002. A fibronectin fragment induces type II collagen degradation by collagenase through an interleukin-1-mediated pathway. *Arthritis Rheum.* **46**:138–148.
39. Weathington, N.M., et al. 2006. A novel peptide CXCR ligand derived from extracellular matrix degradation during airway inflammation. *Nat. Med.* **12**:317–323.
40. Van den Steen, P.E., et al. 2003. Gelatinase B/MMP-9 and neutrophil collagenase/MMP-8 process the chemokines human GCP-2/CXCL6, ENA-78/CXCL5 and mouse GCP-2/LIX and modulate their physiological activities. *Eur. J. Biochem.* **270**:3739–3749.
41. Liu, K., et al. 2006. Successful ovulation in plasminogen-deficient mice treated with the broad-spectrum matrix metalloproteinase inhibitor galardin. *Dev. Biol.* **295**:615–622.
42. Renckens, R., et al. 2006. Endogenous tissue-type plasminogen activator is protective during Escherichia coli-induced abdominal sepsis in mice. *J. Immunol.* **177**:1189–1196.
43. Deindl, E., et al. 2003. Receptor-independent role of the urokinase-type plasminogen activator during arteriogenesis. *FASEB J.* **17**:1174–1176.
44. Yang, Y.H., Carmeliet, P., and Hamilton, J.A. 2001. Tissue-type plasminogen activator deficiency exacerbates arthritis. *J. Immunol.* **167**:1047–1052.
45. Carmeliet, P., et al. 1994. Physiological consequences of loss of plasminogen activator gene function in mice. *Nature.* **368**:419–424.
46. Hoover-Plow, J.L., et al. 2008. Strain and model dependent differences in inflammatory cell recruitment in mice. *Inflamm. Res.* In press.
47. Choi, E.T., et al. 2005. Matrix metalloproteinase-9 modulation by resident arterial cells is responsible for injury-induced accelerated atherosclerotic plaque development in apolipoprotein E-deficient mice. *Arterioscler. Thromb. Vasc. Biol.* **25**:1020–1025.
48. Pyo, R., et al. 2000. Targeted gene disruption of matrix metalloproteinase-9 (gelatinase B) suppresses development of experimental abdominal aortic aneurysms. *J. Clin. Invest.* **105**:1641–1649.
49. Shi, W., et al. 2003. Genetic backgrounds but not sizes of atherosclerotic lesions determine medial destruction in the aortic root of apolipoprotein E-deficient mice. *Arterioscler. Thromb. Vasc. Biol.* **23**:1901–1906.
50. Thompson, R.W., et al. 2006. Pathophysiology of abdominal aortic aneurysms: insights from the elastase-induced model in mice with different genetic backgrounds. *Ann. N. Y. Acad. Sci.* **1085**:59–73.
51. Ducharme, A., et al. 2000. Targeted deletion of matrix metalloproteinase-9 attenuates left ventricular enlargement and collagen accumulation after experimental myocardial infarction. *J. Clin. Invest.* **106**:55–62.
52. Sha, J., et al. 2005. Apo(a) promotes thrombosis in a vascular injury model by a mechanism independent of plasminogen. *J. Thromb. Haemost.* **3**:2281–2289.
53. Chiou, A.C., Chiu, B., and Pearce, W.H. 2001. Murine aortic aneurysm produced by periarterial application of calcium chloride. *J. Surg. Res.* **99**:371–376.
54. Lijnen, H.R., Wagner, E.F., and Collen, D. 1997. Plasminogen-dependent and -independent proteolytic activity of murine endothelioma cells with targeted inactivtion of fibrinolytic genes. *Thromb. Haemost.* **77**:362–367.
55. Davis, V., et al. 1998. Matrix metalloproteinase-2 production and its binding to the matrix are increased in abdominal aortic aneurysms. *Arterioscler. Thromb. Vasc. Biol.* **18**:1625–1633.
56. Goldberg, G.I., Strongin, A., Collier, I.E., Genrich, L.T., and Marmer, B.L. 1992. Interaction of 92-kDa type IV collagenase with the tissue inhibitor of metalloproteinases prevents dimerization, complex formation with interstitial collagenase, and activation of the proenzyme with stromelysin. *J. Biol. Chem.* **267**:4583–4591.